

## Introduction

Austenitic and ferritic stainless steels are the most popular grades, thanks to their good mechanical and corrosion properties, which cover more than 95% of the global stainless steel production. They are mainly used in the Oil and Gas, food, chemical and construction industries.

Stainless steels have a minimum Cr content of 11% that promotes the formation of a coherent, adherent and regenerative layer of chromium oxide ( $Cr_2O_3$ ) on the surface of the steel that protects it from corrosion. When a stainless steel is exposed to relatively high temperatures for long periods of time, the precipitation of various intermetallic compounds and phases can occur. As a result, stress cracking phenomena can occur under stresses, assisted by the presence of hydrogen (H), that is, under states of stress and complex deformations. Also, the phenomena of intergranular corrosion by the formation of  $M_xC_y$  chromium carbides diminish the resistance to corrosion, because in these areas, the atomic H that comes from corrosion reactions, diffuses rapidly through the network towards crystalline imperfections. This causes its sensitization and consequently reduction of its corrosion resistance.

Attention should be paid to the fact that corrosion resistance and mechanical strength are affected when these alloys are exposed to severe working conditions, which can cause localized enrichment of hydrogen on material surface. In general, hydrogen can have a deleterious effect on metals, since only a small amount is enough to promote serious degradation in corrosive and mechanical properties. Second phases play a very important role to understand the hydrogen trapping behavior [1-3] that have a significant effect on possible hydrogen embrittlement mechanism.

## Objective

The objective of this work is to show the effects of different kinds of precipitates acting as hydrogen traps. Thus several thermal treatments considering different cooling conditions were carried out on AISI 316L and AISI 446. Hydrogen cathodic permeation were performed after heat treatments. Finally, microstructural characterization was achieved by optical and scanning electron microscope (SEM).

## Methods

Materials employed, in Figure 1, and its chemical compositions are shown in Table 1.

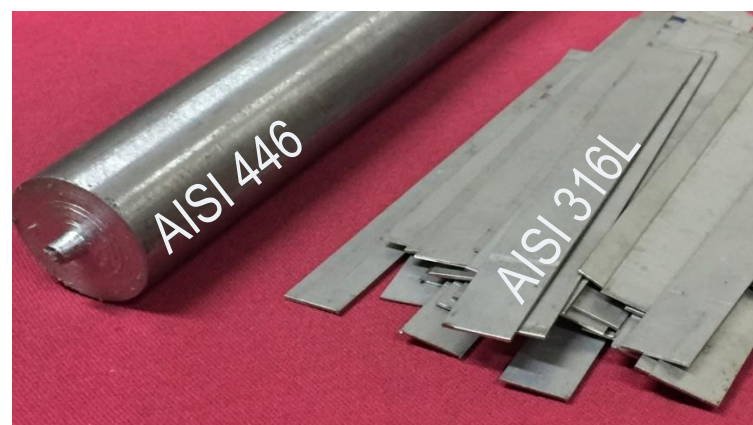


Figure 1: Stainless steels samples

SAMPLE	C	Cr	Ni	Mo	Si
AISI 316L	0,032	17,2	10,7	2,57	0,65
AISI 446	0,058	25,23	0,35	-	0,64

Table 1: Chemical composition in %weight

## Methods

First, adequate thermal treatments were performed to promote carbides precipitation as depicted in Table 2.

SAMPLE	TEMP. (°C)	TIME (MIN.)	ATMOSPHERE	COOLING RATE
AISI 446 (SF1)	850	60	Air	Water
AISI 316L (A1)	900	120	Air	Water
AISI 316L (A2)	900	120	Air	Air

Table 2: Thermal treatments conditions.

Conditions of electrolytic hydrogen permeation cell, Figure 2:

- Anode: graphite
- Current: 35 mA/cm<sup>2</sup>
- Time: 3,5 h
- Solution: 1N H<sub>2</sub>SO<sub>4</sub> + 0,25 g/L NaAsO<sub>2</sub>

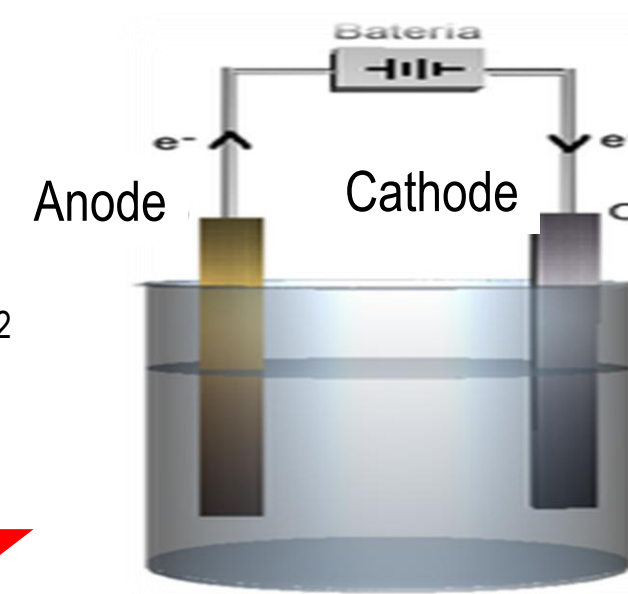
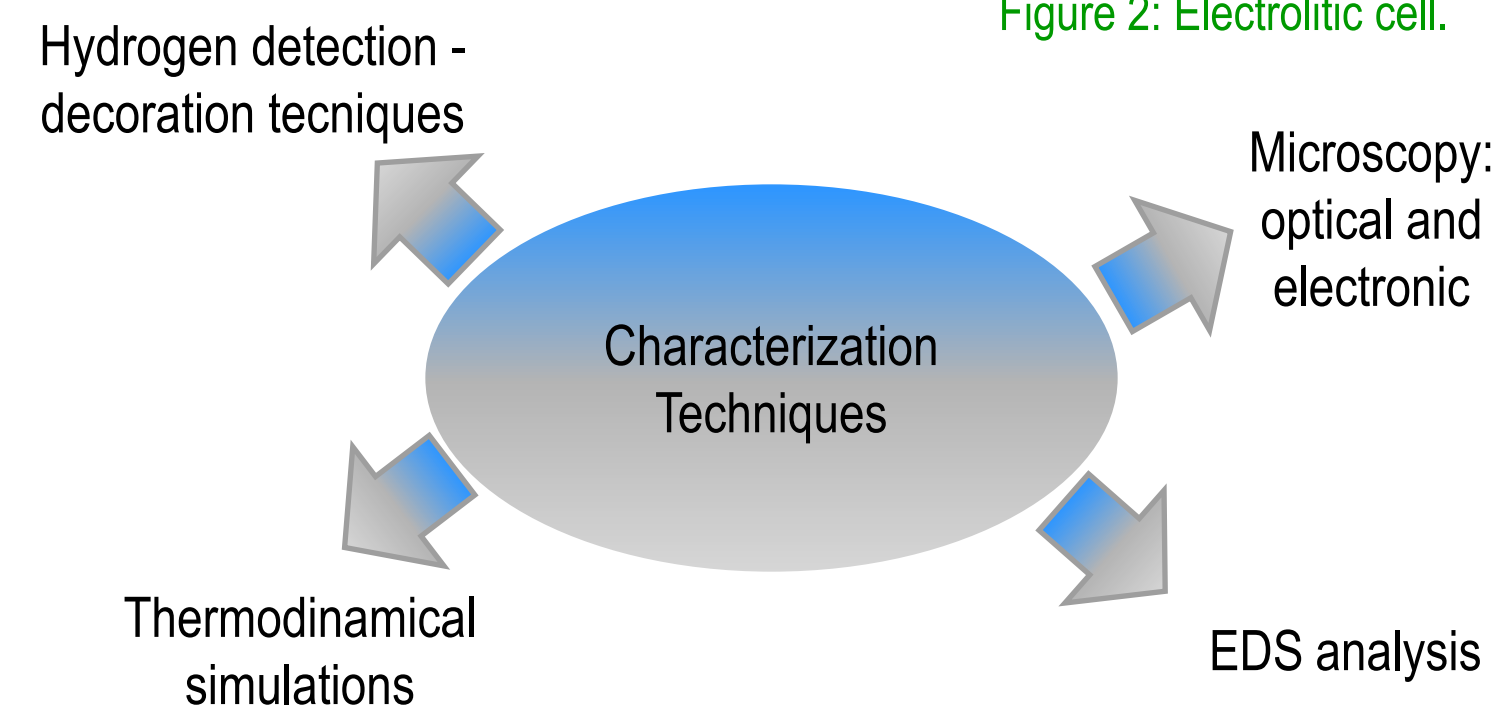


Figure 2: Electrolytic cell.



## Results and Discussion

### As-received steels characterization

Homogeneous distribution of precipitates in both steels, Table 3.

STEELS	CARBIDES	OBSERVATIONS
AISI 316L	22% Cr - 6% Ni and variable contents of Mn, Fe, Mo and Si	Cylindrical (1-4 $\mu$ ) carbides in inter- and transgranular positions, Figure 3a.
AISI 446	39% - 49%Cr	Cylindrical (1-4 $\mu$ ) carbides grouped in colonies.
	65%Cr	Lightly polygonal geometry of carbides with 10-26 $\mu$ long and 12-14 $\mu$ wide, Figure 3b.

Table 3: Description of precipitates that were found on both steels.

## Results and Discussion

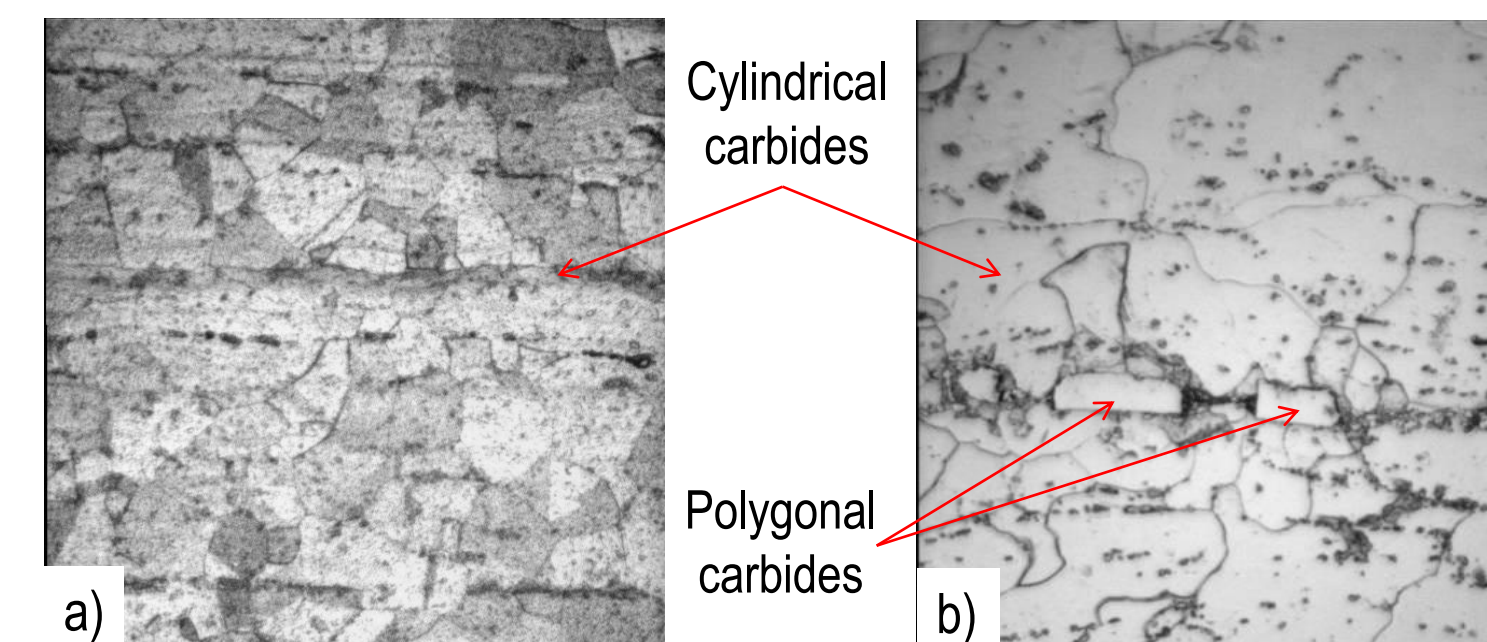


Figure 3: Microstructure of: a) AISI 316L and b) AISI446. [500X]

### Heat treated samples characterization

As a consequence of thermal treatments, isolated distribution of small carbides (1 $\mu$ ) were developed in austenitic stainless steels samples, but forming colonies in the superferritic one. Chemical composition analysis carried out on different types of carbides could determine a decrease in chromium content in all cases in comparison with those precipitates found in the as-received materials. This behaviour was evidenced by semiquantitative analysis of chromium content of each particles. This could be attributed to a chromium depletion from the original carbides towards the austenitic matrix, or attributed to a complex precipitation reaction, [4].

On the other hand, for heat treated samples of AISI 316L (A1 and A2), regardless of the cooling severity, an increase in quantity of precipitates was promoted in relation to the as-received material. Most of them were taken as  $M_{23}C_6$  type carbides, which would be the more stable according to thermodynamic simulation made with FactSage 7.0, [5, 6]. In addition, in sample A2 a continuous gray phase was identified, located at austenitic grain boundaries that again could be  $\gamma$ CrC, FeC, MoC, NiC, CrN, NiN and (Mn, Fe) S in accordance with simulations.

### Hydrogen trapping sites

Silver Decoration Technique [7] was employed to determine possible hydrogen traps. Owing to high hydrogen diffusivity into ferrite phase, sample SF1 showed a great quantity of silver particles (small white particles, Figure 4a) associated with carbides of low chromium content, but there were no trapping effect by particles with high chromium content. Grain boundaries constituted also a secondary hydrogen trapping site for this phase.

On the other hand, in austenitic stainless steels samples (A1 and A2), regardless of cooling condition, a smaller amount of silver particles was observed associated with low chromium content carbides and grain boundaries, Figure 4b.

These differences in hydrogen trapping effect could be explained considering Yu and Perng [8], in concerning with lower diffusivity of H in austenite in contrast with corresponding in ferrite, ie, transport of H depends on the diffusion coefficient of each particular network. The differences in solubilities of H in relation to structures and the trapping sites will be decisive when analyzing the brittle effect of H, [9].

## Results and Discussion

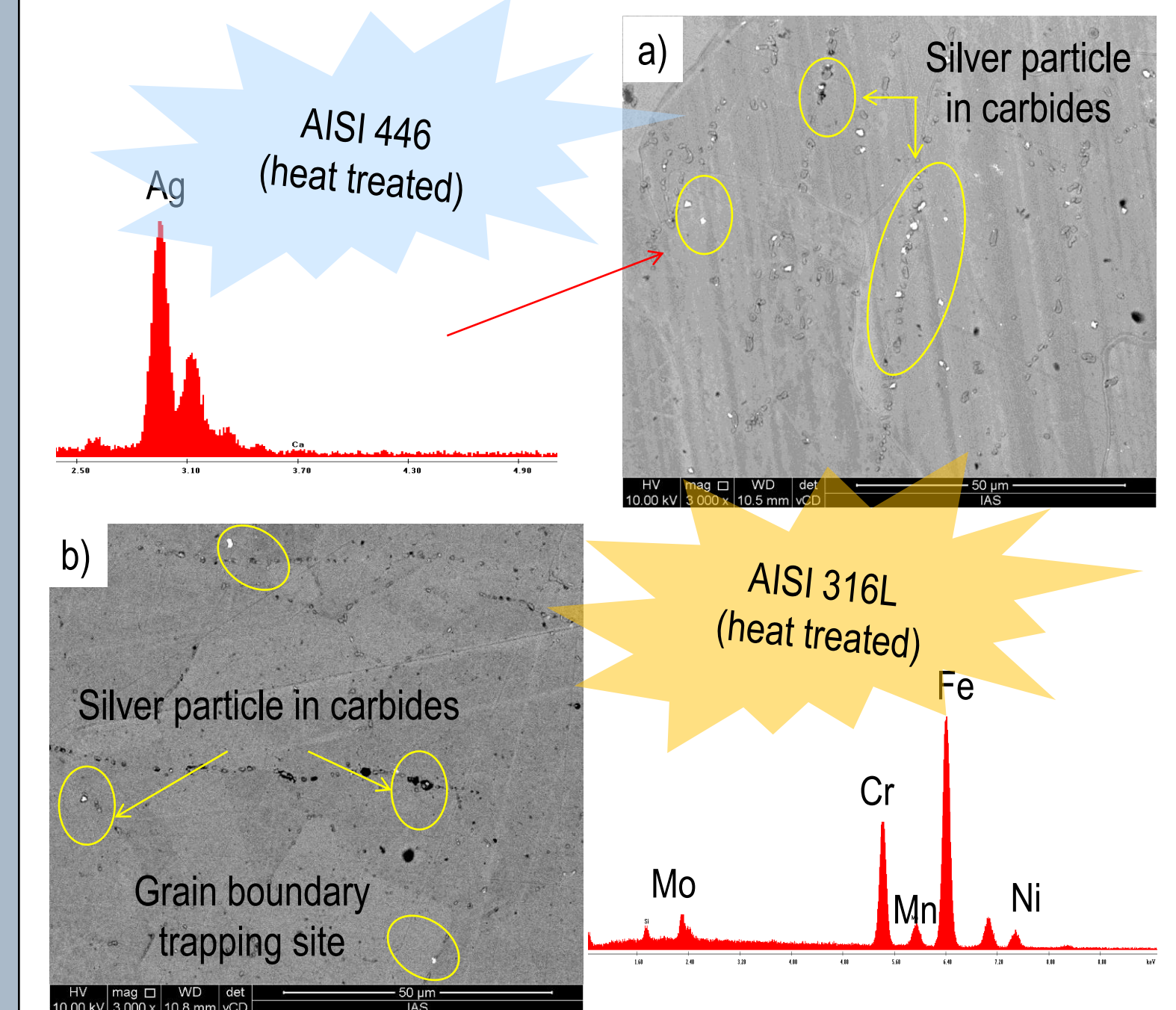


Figure 4: Hydrogen trapping sites.

## Conclusions

The microstructural characterization carried out in both steels allowed to detect a wide variety of carbides, with variable chromium contents and different morphologies. The ferrite-carbide interfaces could be identified as the main hydrogen trap sites in the AISI 446, and the grain boundaries in the AISI 316L.

## References

- [1] Silverstein R., Glam B., Eliezer D., Moreno D., Eliezer S. (2018) Journal of Alloys and Compounds 731:1238-1246.
- [2] Yu C., Shue R.-K., Chen C., Tsay L.-W. (2017) Metals, 7, 58; doi:10.3390/met7020058 2-14.
- [3] Argandoña G., Palacio J. F., Berlanga C., Biezma M. V., Rivero P. J., Peña J., Rodríguez R. (2017) Metals, 7, 219; doi:10.3390/met7060219- 1-12.
- [4] Rozenak P., Eliezer D. (1986) Precipitation behaviour of sensitized AISI type 316 austenitic stainless steel in hydrogen. Journal of Materials Science 21, 3065 – 3070.
- [5] Inés M., Mansilla G. (2017) Efecto de los Tratamientos Térmicos en la Estabilidad de Carburos en Aceros Inoxidables AISI 316 y AISI 446. 17° Congreso Internacional de Metalurgia y Materiales CONAMET-SAM. 18-20 de Octubre de 2018. Copiapó-Chile.
- [6] Inés M., Mansilla G. (2017) Estudio de la precipitación de fases en aceros inoxidables y su interacción con el hidrógeno. 6° Encuentro de Jóvenes Investigadores en Ciencia y Tecnología de Materiales. 17-18 de Agosto de 2017. San Martín, Prov. de Buenos Aires, Argentina.
- [7] Schober, C., Dieker. (1983) Metall. Trans. A.14A, 2440-2442.
- [8] Yu C.L., Perng T.P. (1991) Acta Metall. Mater., 39, 1091-99.
- [9] Singh S., Altstetter C. (1982) Metall. Trans. A, 13A, 1799-1808.